

Measurements of coupled Rayleigh wave propagation in an elastic plate

Boon Wee Ti and William D. O'Brien, Jr.

Electrical and Computer Engineering Department, University of Illinois, Urbana, Illinois 61801

John G. Harris

Theoretical and Applied Mechanics, University of Illinois, Urbana, Illinois 61801

(Received 19 November 1996; accepted for publication 23 May 1997)

At frequencies where the thickness of an elastic plate is more than a wavelength, the propagation of the two lowest Rayleigh–Lamb modes in an elastic plate can be viewed as the propagation of a Rayleigh surface wave over two weakly coupled, surface-wave waveguides. That is, a Rayleigh wave launched on one surface gradually transfers to the other and then back. It does so in a length we call the beatlength. Measurements of the beatlength for brass plates are reported as a function of frequency and thickness. This phenomenon is readily excited and persists over a wide range of thicknesses and frequencies © 1997 Acoustical Society of America.

[S0001-4966(97)05009-1]

PACS numbers: 43.35.Pt, 43.35.Zc, 43.20.Mv [HEB]

INTRODUCTION

The two lowest waveguide modes of an elastic plate can be described as the propagation of a Rayleigh surface wave that starts on one surface, but that gradually transfers to the other surface. It then transfers back to the surface from which it started, the whole cycle taking place over a distance we call the beatlength. Provided the product of wave number and thickness is sufficiently large, one can thus view a plate as two weakly coupled, surface-wave waveguides. The objective of this letter is to report measurements of the beatlength in brass plates. This may be one of the first detailed experimental assessments of this phenomenon, though its possibility has been noted by Auld,¹ Viktorov,² and Brekhovskikh and Goncharov.³ Moreover, Li and Thompson⁴ made similar measurements, but did not widely report them.

The longer service life of structures such as pipelines means that they must be monitored more thoroughly, and over a longer period of time, for damage. Using coupled surface waves may be one way to inspect the inner, and therefore not easily accessible, surface of a pipe from its outer surface. Moreover, if the damage were a small surface-breaking fatigue crack, then a surface wave would readily detect the crack because the surface wave would strike the crack broadside, or if the damage were corrosion, then a surface wave would be more severely attenuated by the patch of corrosion at the surface than a bulk wave. The present measurements indicate that the coupled surface waves are readily excited and detected so that they can be used for such nondestructive testing.

The basic idea is presented using schematic drawings (Figs. 1 and 2). Figure 1 shows the dispersion relation for the two lowest Rayleigh–Lamb modes. The lower curve is that for the lowest antisymmetric mode, while the upper curve is that for the lowest symmetric mode. The vertical axis is the normalized angular frequency (ω multiplied by h/c_t , where h is one-half the thickness of the plate and c_t is the trans-

verse wave speed). The horizontal axis is the normalized wave number (β multiplied by h). The diagonal short-dashed line indicates the straight line formed by $\omega h/c_t$ plotted against $\beta_r h$, where β_r is the Rayleigh wave number. The slope is c_r/c_t , where c_r is the Rayleigh wave speed. In the neighborhood of the intersection points of the horizontal, long-dashed line with the dispersion curves, the x particle displacements look roughly as sketched schematically in Fig. 2. If the symmetric and antisymmetric modes are both excited in phase, then the sum approximates a Rayleigh wave on the upper surface. This is indicated by the solid line in Fig. 2(c). However, each mode propagates with a slightly different wave number, β_s for the symmetric mode and β_a for the antisymmetric mode. After a distance $L/2$, the two modes move π out of phase. Adding the two modes together at this location approximates a Rayleigh wave on the lower surface. This is indicated by the dashed line in Fig. 2(c). After propagating an additional distance $L/2$, the modes move back into phase (more accurately 2π out of phase) and their sum again approximates a Rayleigh wave, now on the upper surface. In this sense the propagation of the two modes can be viewed as a Rayleigh surface wave coupling from one surface-wave waveguide to another. Figure 1, by means of the vertical dashed lines, indicates the difference 2ε between the wave numbers β_s and β_a . The difference between β_s and β_r is almost equal to that between β_r and β_a . The beatlength L of the coupled waves is that distance over which the two modes move out of phase by 2π , that is,

$$(\beta_a - \beta_s)L = 2\pi \quad (1)$$

or

$$L/h = \pi/h\varepsilon. \quad (2)$$

With Eq. (5.15), Brekhovskikh and Goncharov³ give an estimate of ε for large βh . However, we use the exact Rayleigh–Lamb dispersion relation⁵ to calculate ε and L/h .

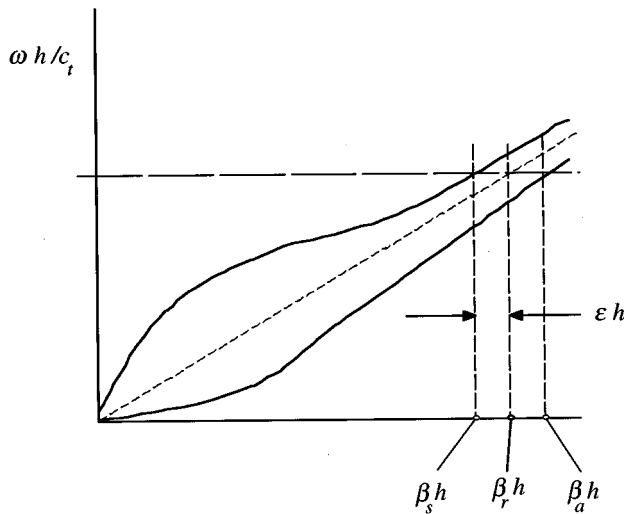


FIG. 1. A sketch of the dispersion relation for the two lowest modes of an elastic plate. The upper curve is the symmetric mode and the lower is the antisymmetric mode. The beatlength $L = \pi/\epsilon$. Figure 2 sketches the particle displacement in the neighborhood of the intersections of the long-dashed horizontal line with the dispersion curves.

I. MEASUREMENTS

The longitudinal and shear wave speeds in brass are experimentally determined using standard pulse-echo techniques with a Panametrics 5800 Pulser/Receiver. From the acquired front and back wall echoes, the time difference between these echoes was calculated with a correlation procedure and, using the measured plate thickness, the wave speed was calculated.⁶ The longitudinal wave speed is found using a 15-MHz Panametrics V319 immersion transducer. The shear wave speed is found using a 20-MHz Panametrics V222-BA-RM normal incidence, shear-wave, contact transducer.

The view, from above, of the experimental arrangement is sketched in Fig. 3. A focused 3-MHz Panametrics V3680 transducer directs a focused ultrasonic beam at the surface of a 2.38-mm-thick brass plate at the Rayleigh angle θ_r . Because we were imitating a possible nondestructive testing measurement we did not measure the plate's thickness systematically, using a micrometer (accuracy about $\pm 13 \mu\text{m}$) to measure the thickness at only one or two locations. At 3 MHz the longitudinal wavelength, in the brass plate, is approximately 1.5 mm and the shear wavelength approximately one-half that. The coupling phenomena we were seeking would be of little use in nondestructive testing if it were sensitive to variations in thickness on the order of 1/100 of a wavelength.

The plate is partially submerged in water. The portion submerged in water is used to position the transducer relative to the plate surface via pulse-echo, normal incidence, time-of-flight measurements. That above water is used to make the beatlength measurements. There the sound is coupled to the plate by a jacket of water that surrounds the sound beam, as shown in Fig. 3. The portion of the plate, in air, experiences no substantial fluid loading. The same function generator was used for the positioning measurements and the beat-

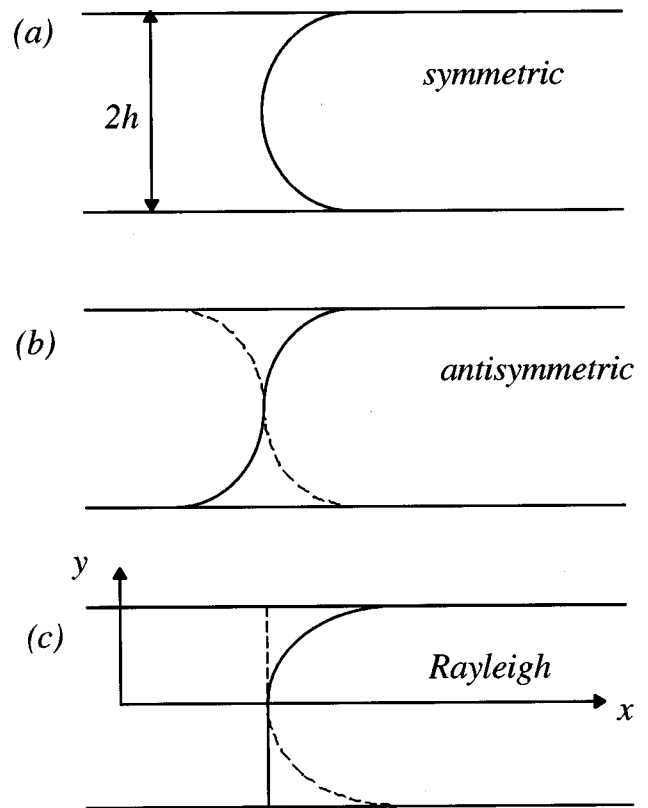


FIG. 2. A sketch of the x particle displacements corresponding to the neighborhoods of the intersection of the long-dashed horizontal line in Fig. 1 with each dispersion curve. The solid lines indicate that the modes are in phase, while the dashed lines indicate that they are π out of phase: (a) symmetric mode, (b) antisymmetric mode, and (c) algebraic sum of the two modes (schematic only).

length measurements, with only the gate length being changed.

The normal beam axis to the brass plate is found by adjusting the focused transducer to an angle where the reflection, measured using the pulse-echo mode, is maximum. The parallelism of the plate to the scanning motion of the transducer was adjusted by using the same pulse-echo measurement to measure the distance at a few randomly selected points, on that part of the plate submerged in water, to make the distances equal. The precision positioning system is computer controlled and has a linear accuracy of about $5 \mu\text{m}$. Assuming that the parallelism was maintained to $\pm \frac{1}{4}$ of a wavelength, in water at 3 MHz, the accuracy would be $\pm 0.12 \text{ mm}$. The transducer is then rotated to the Rayleigh angle θ_r . This angle is calculated (see Sec. III) from the measured wave speeds. The rotational accuracy of the precision positioning system, also computer controlled, is about 0.02° .

The beatlength is experimentally determined as follows. With the incident beam at the Rayleigh angle and the focal point on the metal plate, the transmitter is moved parallel to the plate surface, toward the broadband receiver, a Deci model SE 1025-H308 surface contact transducer. The area of the intersection of the beam with the plate's surface is not

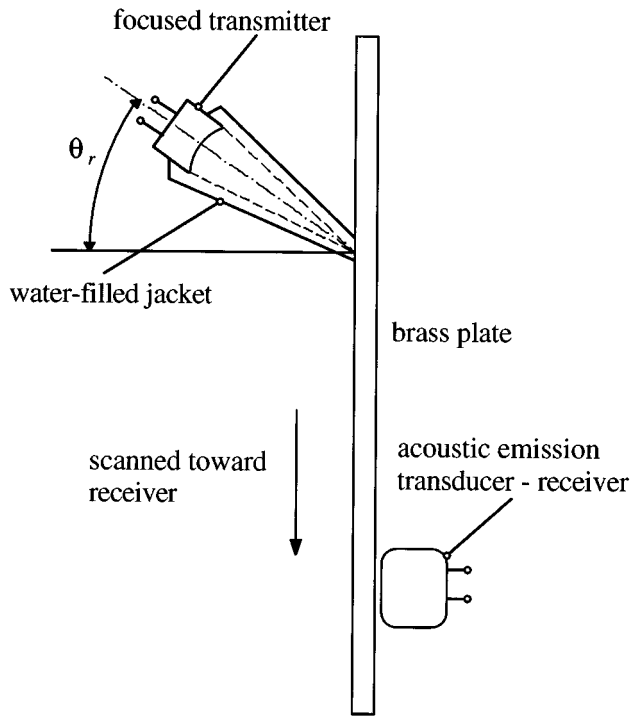


FIG. 3. A drawing of the experimental arrangement viewed from above. The central axis of the focused transducer makes an angle θ_r with the vertical. The sound is coupled to the plate by means of a water-filled jacket. Though the lower part of the plate is in water (this is not shown), the part used for the beatlength measurement is loaded only by the surrounding air. The focal point is placed at the plate surface and moved toward the stationary receiving transducer.

important beyond the need to keep it small so that the plate is not fluid loaded. The transmitter is moved in $200 \mu\text{m}$ intervals, and at each interval, a 10-MHz A/D rate, 1024-point data record of the temporal, received sinusoidal signal is recorded by the receiver. The rms value for each position is calculated and recorded.

The transmitter is moved a distance slightly greater than three times the estimated beatlength. The rms values for each position are Fourier transformed without windowing using a 4096 FFT. The power spectrum is calculated to determine the peak corresponding to the beatlength.

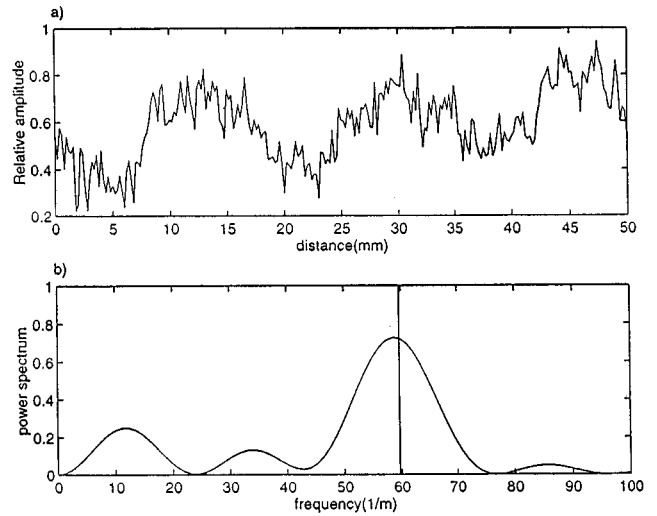


FIG. 4. Representative data, case 4 of Table I. (a) The spatially amplitude-modulated, received signal plotted against position along the plate's surface (500 rms data points, 100-mm scan distance). (b) The power spectrum of the signal from (a) plotted against the spatial frequency (1/distance). The vertical line indicates the theoretically estimated, spatial beat frequency.

II. RESULTS

The measured longitudinal wave speed in brass is 4536 m/s. The measured shear wave speed in brass is 2215 m/s. Their ratio is 2.048. The measured wave speeds had an accuracy of about $\pm 0.1\%$.

Figure 4 shows a typical measurement (case 4 of Table I). Figure 4(a) shows a single realization of the amplitude modulated signal from a 100-mm scan, that is, the transmitter was moved 100 mm, in $200\text{-}\mu\text{m}$ intervals, toward the receiver. Figure 4(b) shows the spatial power spectrum of the signal from Fig. 4(a). The higher spatial frequency components evident in Fig. 4(a) are outside of the spatial frequency range of Fig. 4(b). The vertical line marks the theoretically predicted spatial beat frequency calculated using the exact Rayleigh-Lamb dispersion relation.⁵

Figure 5 plots L/h against $\omega h/c_t$. The error bars represent $\pm 10\%$ of a theoretically predicted value. The transmitter's operating frequency f is varied to produce the seven different $\omega h/c_t$ cases (Table I).

Table I summarizes the results of the experiment conducted on brass. The wave number β must be greater than ϵ

TABLE I. The measured and calculated values of the important parameters. The temporal frequency f is the transducer operating frequency, f_a is the spatial frequency, L is the beatlength, and h is the half-thickness of the brass plate. Note that case 4 is illustrated in Fig. 4.

Case	f (MHz)	$\omega h/c_t$	β/ϵ	Theory			Experiment		
				f_a (m^{-1})	L (mm)	L/h	f_a (m^{-1})	L (mm)	L/h
1	0.733	2.59	6.88	109.8	9.1	7.6	97.7	10.2	8.6
2	0.800	2.82	7.64	88.9	11.3	9.4	80.6	12.4	10.4
3	0.866	3.06	13.01	72.3	13.8	11.6	63.5	15.7	13.2
4	0.933	3.29	17.14	59.7	16.7	14.1	58.6	17.1	14.4
5	1.00	3.53	22.11	50.0	20.0	16.8	45.2	22.1	18.6
6	1.20	4.23	43.73	30.8	32.5	27.3	28.1	35.6	29.9
7	1.33	4.70	66.03	22.9	43.7	36.7	22.0	45.5	38.2

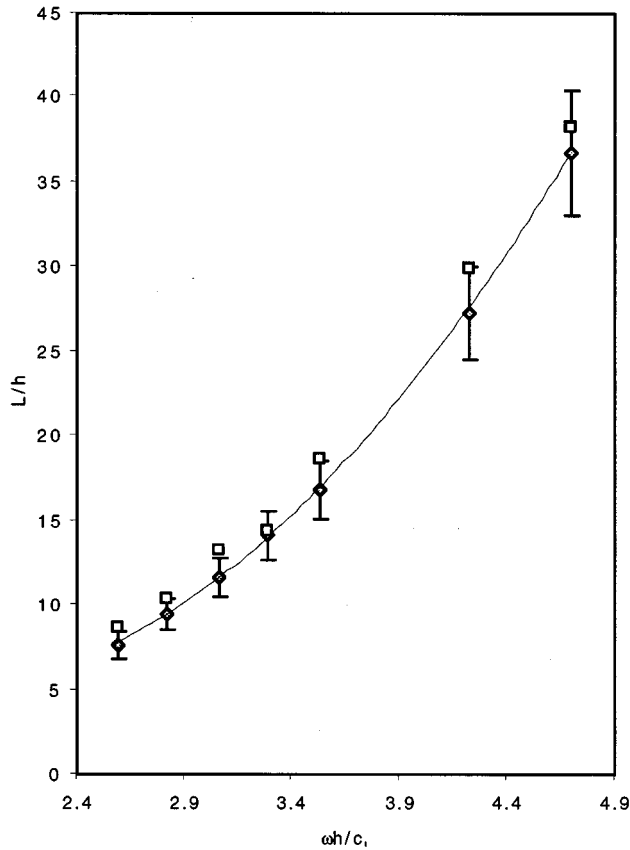


FIG. 5. A plot of L/h against $\omega h/c_r$. The data points indicated by open squares are the measured results. The data points indicated by open diamonds are the theoretically predicted results. A $\pm 10\%$ error bar is attached to the theoretically estimated results.

to produce a spatially modulated signal. Thus β/ε is recorded. The theoretical value for L/h is calculated from the exact dispersion relations. The experimentally determined spatial beat frequency, beatlength, and normalized beatlength are tabulated in the last three columns. While earlier we indicated, to some extent, the accuracy of our measurements, we have not done so in this table because the measurement we sought was not sensitive to these inaccuracies.

III. DISCUSSION

The Rayleigh angle, θ_r , is defined as

$$\theta_r = \sin^{-1}(c/c_r), \quad (3)$$

where c is the speed of sound in water ($c = 1482$ m/s at 20°C). A very good approximation for c_r is⁷

$$c_r/c_t = (0.87 + 1.12\nu)/(1 + \nu), \quad (4)$$

where

$$\nu = [(c_l/c_t)^2 - 2]/2[(c_l/c_t)^2 - 1]. \quad (5)$$

From the measured values of c_l and c_t , Eq. (4) gives $c_r = 2069$ m/s and Eq. (3) gives $\theta_r = 45.78^\circ$. This is the angle used in these measurements.

Figure 4(b) suggests that the beat phenomenon is robust in the spatial frequency domain, and that the measured spatial frequency is in agreement with theory (see Table I). Figure 5 indicates that the measured values of the spatial beat frequency lie close to or within $\pm 10\%$ of the theoretically predicted values. Brekhovskikh and Goncharov³ suggest that βh must be large for the coupling phenomena to be clearly observed and their estimate of ε assumes this. However, our values of βh ranged from 2 to 5, and yet we observe the coupling phenomena without difficulty. Moreover, the beatlengths indicate that the use of the coupled waves to access an inner surface is realistic. None of the beatlengths is so great that the signals would become too severely attenuated, with distance, to carry information from the far surface.

Initially, we had been concerned that, in addition to the two lowest modes, we might excite higher modes and as a consequence some power would be carried by them and lost to the coupling phenomenon. This appears not to be the case suggesting that when we are incident at the Rayleigh angle we strongly excite only the two lowest modes.

ACKNOWLEDGMENTS

The support of American Chemical Society (Petroleum Research Fund) Grant PRF 29555-AC9 for this work is gratefully acknowledged. Boon Wee Ti also thanks the Economic Development Board of Singapore for providing a scholarship to study at UIUC.

- ¹B. A. Auld, *Acoustic Fields and Waves in Solids* (Krieger, Malabar, FL, 1990), Vol. 2, pp. 93–94.
- ²I. A. Viktorov, *Rayleigh and Lamb Waves* (Plenum, New York, 1967), pp. 93–96.
- ³L. Brekhovskikh and V. Goncharov, *Mechanics of Continua and Wave Dynamics* (Springer-Verlag, New York, 1985), pp. 75–81. Note that the first of Eqs. (5.16) has a sign error. The plus sign between the two terms should be replaced by a minus sign.
- ⁴Private communication, R. B. Thompson, Iowa State University.
- ⁵B. A. Auld, *Acoustic Fields and Waves in Solids* (Krieger, Malabar, FL, 1990), Vol. 2, pp. 77–82, Eqs. (10.18) and (10.19).
- ⁶I. A. Hein and W. D. O'Brien, Jr., "A real-time ultrasound time-domain correlation blood flowmeter, part II, performance and experimental verification," *IEEE Trans. Ultrason. Ferroelectr. Freq. Control* **40**, 776–785 (1993).
- ⁷I. A. Viktorov, *Rayleigh and Lamb Waves* (Plenum, New York, 1967), p. 3.